International Journal of Scientific Research in Mathematical and Statistical Sciences
Volume-4, Issue-5, pp.17-26, October (2017)
Research Paper
E-ISSN: 2348-4519

Numerical Study Of an Unsteady 2-D Compressible Inviscid Flow with Heat Transfer with Slip Boundary Conditions Using MacCormack Technique

Arti Kaushik

Department of Mathematics, Maharaja Agrasen Institute of Technology, Delhi, India

Corresponding Author: arti.kaushik@gmail.com

Available online at: www.isroset.org

Received 14th Sep 2017, Revised 17th Sep 2017Accepted 24th Oct 2017, Online 30th Oct 2017

Abstract- In this paper the problem of an unsteady 2-D compressible inviscid flow with heat transfer with slip boundary conditions is analyzed. Numerical solutions of the governing equations are obtained by using Mac Cormack technique. The numerical computations of *u*-velocity, *v*-velocity, pressure and temperature are done at different times for different positions along *x*- axis and *y*- axis. The numerical solutions of the *u*-velocity, *v*-velocity, pressure and temperature obtained in this analysis have been ensured to be stable based on stability requirements. The significant findings from the present analysis have been given under conclusion.

Keywords- Inviscid flow, Heat transfers, Euler's equations, MacCormack technique, slips boundary conditions.

I. INTRODUCTION

The study of fluid flow and heat transfer has been receiving the attention of many researchers due to its wide applications in industry and technological fields such as cooling of electronic components, solar collectors, casting and welding of manufacturing processes, oil recovery process, geothermal extraction etc. MacCormack technique is an important tool used in the study of incompressible fluid flow with heat transfer. The scheme has been extensively used, modified and developed over the years. It was first introduced in 1969[1] and became the most popular explicit finite-difference method for solving fluid flows. Bernard[2] extended Mac Cormack scheme for incompressible flow on marker and cell grid. Payri, Torregrosa and Chust[3] used MacCormack technique to solve 1-D flow equations in case of exhaust system of single cylinder engine. Hixon and Turkel [4] derived a new class of high accuracy compact MacCormack technique. Later, they extended [5] MacCormack technique to implicit differencing scheme and developed a new class of high order accurate scheme. Perrin and Hu [6] used MacCormack scheme for nearly incompressible Newtonian fluid. Guoyuan and Jackson [7] revised both MacCormack and Saulyev methods for dynamic 1-D advection-dispersion –reaction equation and greatly improved the prediction accuracy over the original ones. Pochai [8] studied two models both formulated in 1-D and proposed a modified MacCormack technique. Das and Bagheri [9] used MacCormack technique to solve a 2-D shallow water equations. Gallagher et al. [10] proposed two modifications leading to the formation of generalized MacCormack scheme within a dual time framework.

In view of available literature mentioned above, it can be seen that MacCormack technique has been used quite often to compute unsteady, compressible as well as incompressible flows. This technique has been extensively used to obtain time accurate solution for fluid flow. This technique is a simpler variant of Lax-Wandroff technique which is basically a two step technique with second order accuracy in both space and time. MacCormack technique is computationally efficient, easy to implement and second order accurate in both space and time and is appropriate to obtain reliable results. However, a disadvantage of the MacCormack method is that computations involving the compressible N-S equations sometimes become unstable because of numerical oscillations, which arises due to inadequate mesh refinement in regions of large gradients. But, in many cases, it is infeasible to refine the mesh in these regions, because of the substantially higher computing

needs. So in these cases, errors due to numerical oscillations are inevitable

The calculation of compressible flow models is significantly different from incompressible flow models. The most important difference is the addition of a time derivative to the continuity equation and also the addition of one unknown i.e. the density. The compressible flow models has not been studied widely by the researchers due to the complexity involved in computing four unknown variables *u, v, p, T* simultaneously. In the present study, we adopt MacCormack technique to numerically investigate an unsteady 2-D compressible inviscid flow with heat transfer with slip boundary conditions. The paper is organized as follows: In Section II, we introduce governing equations, initial and boundary conditions under mathematical formulation. The computational procedure and algorithm has been detailed under Section III. The numerical computations of *u, v, P, T* for various test cases has been given under Section IV. Results and discussions have been given under Section V. Conclusions of this study have been summarized in the final section.

II. MATHEMATICAL FORMULATION

We consider an unsteady, 2D inviscid flow with heat transfer with slip boundary conditions. Let this flow passes through a rectangular cavity as shown in Figure1. All fluid properties are assumed to be constant. We assume no body forces and no volumetric heat addition. Under these assumptions, the 2D compressible, inviscid Euler's equations in dimensionless form are given by:

Continuity: $$\frac{\partial \rho}{\partial t} = -\left(\rho \frac{\partial u}{\partial x} + u \frac{\partial \rho}{\partial x} + \rho \frac{\partial v}{\partial y} + v \frac{\partial \rho}{\partial y} \right) \quad (1)$$

X momentum:

$$\frac{\partial u}{\partial t} = -\left(u \frac{\partial u}{\partial x} + v \frac{\partial u}{\partial y} + \frac{1}{\rho} \frac{\partial p}{\partial x} \right) \quad (2)$$

Y momentum:

$$\frac{\partial v}{\partial t} = -\left(u \frac{\partial v}{\partial x} + v \frac{\partial v}{\partial y} + \frac{1}{\rho} \frac{\partial p}{\partial y} \right) \quad (3)$$

Energy:

$$\frac{\partial T}{\partial t} = -\left(u \frac{\partial T}{\partial x} + v \frac{\partial T}{\partial y} + \frac{p}{\rho} \frac{\partial u}{\partial x} + \frac{p}{\rho} \frac{\partial v}{\partial y} \right) \quad (4)$$

With the initial and boundary conditions:

For *t = 0 :* *u(x,y,0)=0, v(x,y,0)=0, T(x,y,0)=0, p(x,y,0)=10, ρ(x,y,0)=10*

For *t > 0 :*

At the wall AB : $x = 0 \; ; \; 0 \le y \le 1; v = 10; T = 20; \; \rho = 10; p = 10$ At the wall BC : $y = 0 \; ; \; 0 \le x \le 1; u = 10; T = 10; \rho = 10, p = 10$ At the wall CD : $x = 1 \; ; \; 0 \le y \le 1; v = 10; T = 20; \rho = 10; p = 10$ At the wall DA : $y = 1 \; ; \; 0 \le x \le 1; u = 10; T = 10; \rho = 10; p = 10$

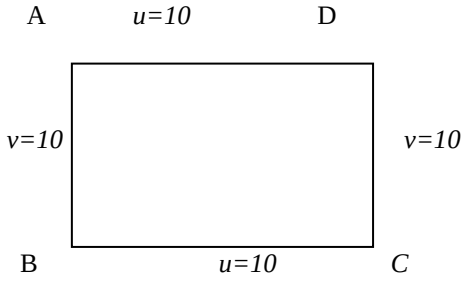

Fig. 1 Rectangular Cavity

III. COMPUTATIONAL PROCEDURES AND ALGORITHMS

In order to solve Eqns. (1)-(4) using MacCormack technique, we consider a two-dimensional grid as shown in Fig. 2.We assume that the flow field at each grid point in Fig. 2 is known at time t, and we proceed to calculate the flow-field variables at the same grid points at time $t + \Delta t$, as illustrated in Fig. 3.To start with, we first find predicted values of the variables as follows:

Predictor Step: In the right-hand side of Eqn. (1), we replace the spatial derivatives with forward differences.

$$\left(\frac{\partial \rho}{\partial t}\right)_{i,j}^{t} = -\left(\begin{array}{l} \rho_{i,j}^{t}\,\dfrac{u_{i+1,j}^{t}-u_{i,j}^{t}}{\Delta x} + u_{i,j}^{t}\,\dfrac{\rho_{i+1,j}^{t}-\rho_{i,j}^{t}}{\Delta x} + \\ \rho_{i,j}^{t}\,\dfrac{v_{i,j+1}^{t}-v_{i,j}^{t}}{\Delta y} + v_{i,j}^{t}\,\dfrac{\rho_{i,j+1}^{t}-\rho_{i,j}^{t}}{\Delta y} \end{array}\right) \quad (5)$$

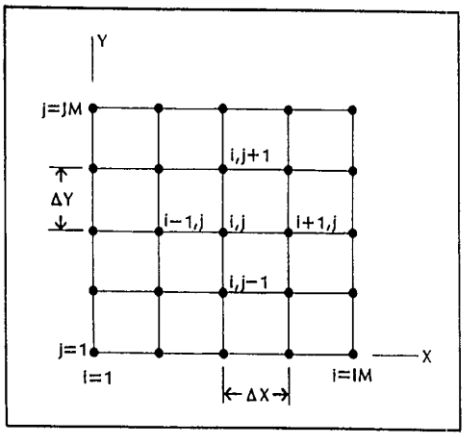

Fig. 2: Rectangular Grid Segment

All the flow variables on right-hand side of Eqn. (5) are known at time t. Now, we obtain the predicted value of density $\left(\overline{\rho}\right)^{t+\Delta t}$, from first two terms of a Taylor's series, as follows

$$\left(\overline{\rho}\right)_{i,j}^{t+\Delta t} = \rho_{i,j}^{t} + \left(\frac{\partial \rho}{\partial t}\right)_{i,j}^{t} \Delta t \qquad (6)$$

In the same way, we obtain the predicted values for *u, v* and *T*, i.e.

$$\left(\overline{u}\right)_{i,j}^{t+\Delta t} = u_{i,j}^{t} + \left(\frac{\partial u}{\partial t}\right)_{i,j}^{t} \Delta t \qquad (7)$$

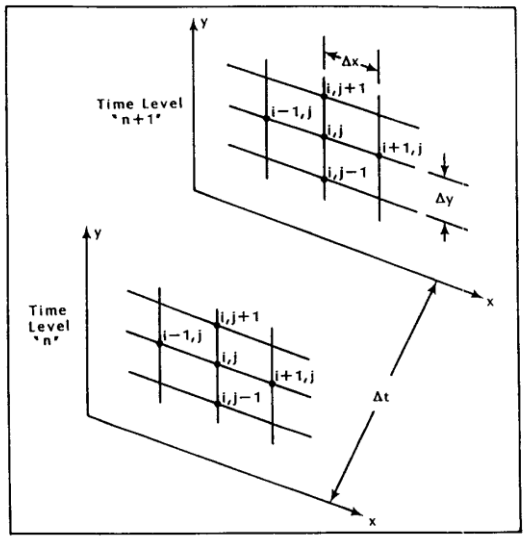

Fig. 3: A schematic for the grid for time marching

$$\left(\overline{v}\right)_{i,j}^{t+\Delta t} = v_{i,j}^{t} + \left(\frac{\partial v}{\partial t}\right)_{i,j}^{t} \Delta t \qquad (8)$$

$$\left(\overline{T}\right)_{i,j}^{t+\Delta t} = T_{i,j}^{t} + \left(\frac{\partial T}{\partial t}\right)_{i,j}^{t} \Delta t \qquad (9)$$

Corrector Step: In this step, we substitute the predicted values of ρ, u, v (obtained from Eqns. (6)-(8)) in Eqn. (1) and obtain the predicted values of the time derivative of ρ at time $t + \Delta t$, i.e.

$$\left(\frac{\overline{\partial \rho}}{\partial t}\right)_{i,j}^{t+\Delta t} = -\left(\begin{array}{l} \left(\overline{\rho}\right)_{i,j}^{t+\Delta t}\,\dfrac{\left(\overline{u}\right)_{i,j}^{t+\Delta t} - \left(\overline{u}\right)_{i-1,j}^{t+\Delta t}}{\Delta x} + \\ \left(\overline{u}\right)_{i,j}^{t+\Delta t}\,\dfrac{\left(\overline{\rho}\right)_{i,j}^{t+\Delta t} - \left(\overline{\rho}\right)_{i-1,j}^{t+\Delta t}}{\Delta x} \\ + \left(\overline{\rho}\right)_{i,j}^{t+\Delta t}\,\dfrac{\left(\overline{v}\right)_{i,j}^{t+\Delta t} - \left(\overline{v}\right)_{i,j-1}^{t+\Delta t}}{\Delta y} + \\ \left(\overline{v}\right)_{i,j}^{t+\Delta t}\,\dfrac{\left(\overline{\rho}\right)_{i,j}^{t+\Delta t} - \left(\overline{\rho}\right)_{i,j-1}^{t+\Delta t}}{\Delta y} \end{array}\right) \quad (10)$$

Here, we are using backward differencing for spatial derivatives. Similarly, using predicted values of ρ, u, v

and T, we obtain the predicted values of the time derivative of u, v and T at time $t+\Delta t$, i.e. $\left(\overline{\frac{\partial u}{\partial t}}\right)_{i,j}^{t+\Delta t}$, $\left(\overline{\frac{\partial v}{\partial t}}\right)_{i,j}^{t+\Delta t}$ and $\left(\overline{\frac{\partial T}{\partial t}}\right)_{i,j}^{t+\Delta t}$.

It can be seen that forward differences are used for all spatial derivatives in the predictor step, while backward differences are used in the corrector step. The forward and backward differencing can be alternated between predictor and corrector steps as well. This provides a higher accuracy and stability for non-linear problems including the one at hand.

Next, we obtain the average value of time derivative of ρ at time $t+\Delta t$ using

$$\left(\frac{\partial \rho}{\partial t}\right)_{av} = \frac{1}{2}\left[\left(\frac{\partial \rho}{\partial t}\right)_{i,j}^{t} + \left(\overline{\frac{\partial \rho}{\partial t}}\right)_{i,j}^{t+\Delta t}\right] \qquad (11)$$

The final corrected value of density at $t+\Delta t$ is obtained as

$$\rho_{i,j}^{t+\Delta t} = \rho_{i,j}^{t} + \left(\frac{\partial \rho}{\partial t}\right)_{av} \Delta t \qquad (12)$$

In the similar fashion, we obtain the corrected values of *u*, *v* and *T*, using

$$u_{i,j}^{t+\Delta t} = u_{i,j}^{t} + \left(\frac{\partial u}{\partial t}\right)_{av} \Delta t \qquad (13)$$

$$v_{i,j}^{t+\Delta t} = v_{i,j}^{t} + \left(\frac{\partial v}{\partial t}\right)_{av} \Delta t \qquad (14)$$

$$T_{i,j}^{t+\Delta t} = T_{i,j}^{t} + \left(\frac{\partial T}{\partial t}\right)_{av} \Delta t \qquad (15)$$

Following these predictor-corrector steps we obtain the values of variables ρ, u, v and *T* at grid point (*i,j*) at time $t+\Delta t$.These steps are repeated at all grid points to obtain the values of variables at all grid points (*i,j*) at time $t+\Delta t$.

IV. NUMERICAL COMPUTATIONS

In order to obtain the unknown variables, ρ, u, v and *T*, numerical computations are carried out at different time intervals and displayed. While doing the computations, we have taken $\Delta x = 0.1,\ \Delta y = 0.1,\ \Delta t = 0.0001$. The computations of *u*-velocity, *v*-velocity, density and temperature are done by following the MacCormack technique which has been described under Section 3. The same algorithm has been implemented in MATLAB programming language. The unknown quantities are obtained at different node points and at different time intervals. The computed values of unknown quantities *u*-velocity, *v*-velocity, pressure and temperature at different nodes and different time intervals are given under Tables 1 to 4.

The *u*-velocity for different times 0.005, 0.010, 0.015 and 0.020, at different positions along *x*-axis and *y*-axis have been computed and given under Table 1.

The numerical values of *u*-velocity of the fluid at different times 0.005, 0.010, 0.015 and 0.020 are illustrated in Figures 4 to 7.The numerical values of *u*-velocity at different positions 0.3and 0.9 along x-axis but at different times 0.005, 0.010, 0.015 and 0.020 are illustrated in Figures 8 to 9. The numerical values of *u*-velocity at *x*=0.6 have negligible difference from values of *u*-velocity at *x*=0.3.

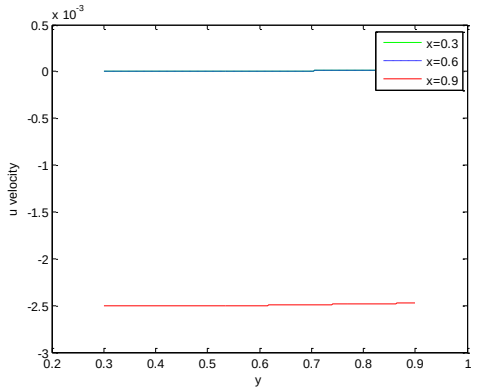

Fig 4:u-velocity at t=0.005

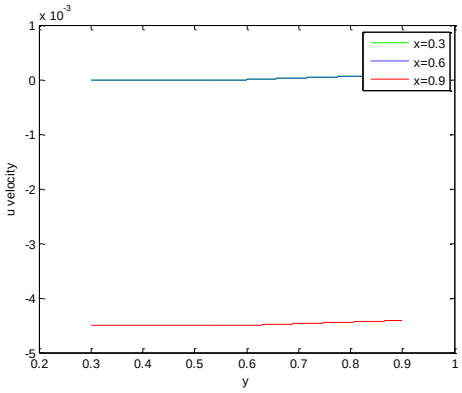

Fig. 5: u-velocity at t=0.010

The numerical values of *v*-velocity of the fluid at different times 0.005, 0.010, 0.015 and 0.020 are illustrated in Figures 10 to 13. The numerical values of *v*-velocity at different positions 0.3, and 0.9 along y-axis but at different times 0.005, 0.010, 0.015

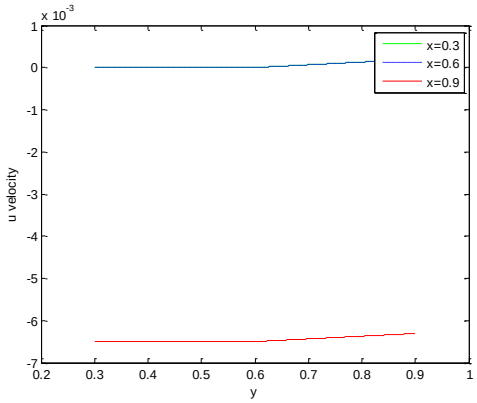

Fig 6: u-velocity at t=0.015

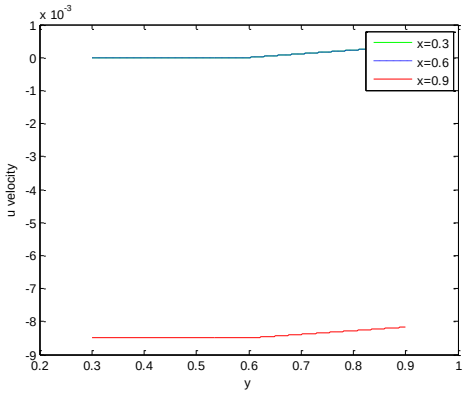

Fig 7: u-velocity at t=0.020

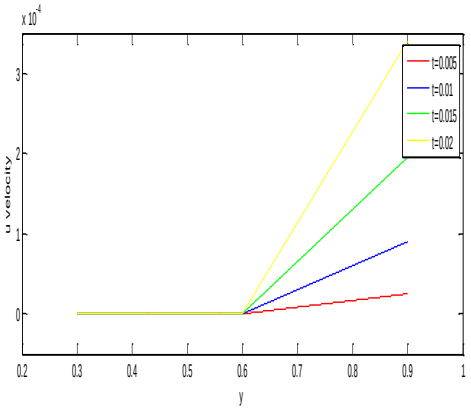

Fig. 8: u-velocity at x=0.3

and 0.020 are illustrated in Figures 14 to 15. The numerical values of *v*-velocity at *y*=0.6 have negligible difference from values of *v*-velocity at *y*=0.3

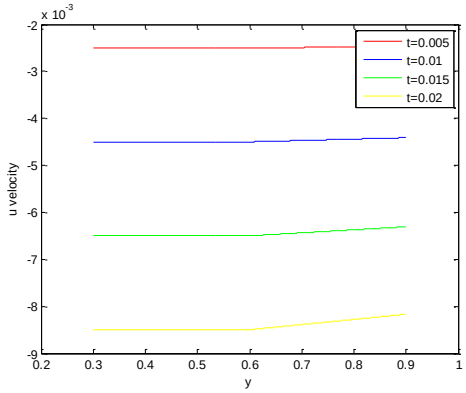

Fig 9 u-velocity at x=0.9

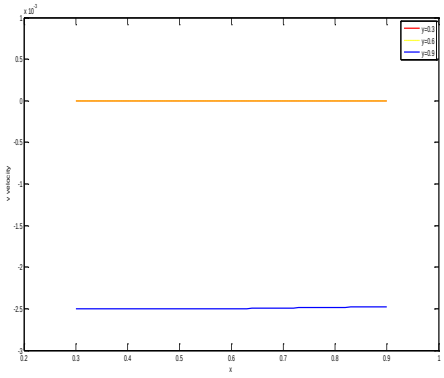

Fig 10: v-velocity at t=0.005

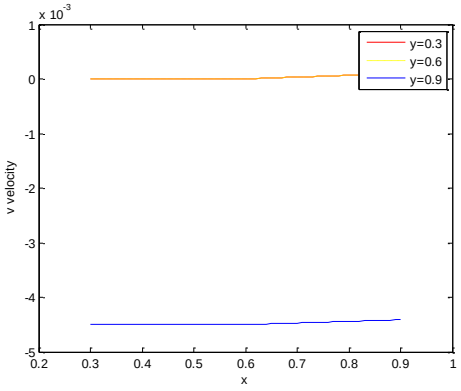

Fig11: v-velocity at t=0.010

The numerical solutions for the pressure at different times 0.005, 0.010, 0.015 and 0.020 for values of *x* as 0.3, 0.6 and 0.9 and for values of *y* as 0.3, 0.6 and 0.9 have been computed and given in Table 3. The pressure of the fluid at different times 0.005, 0.010, 0.015 and 0.020 is illustrated in Figures 16 to 19.

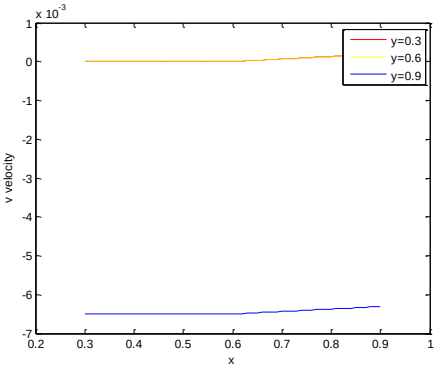

Fig. 12: v-velocity at t=0.015

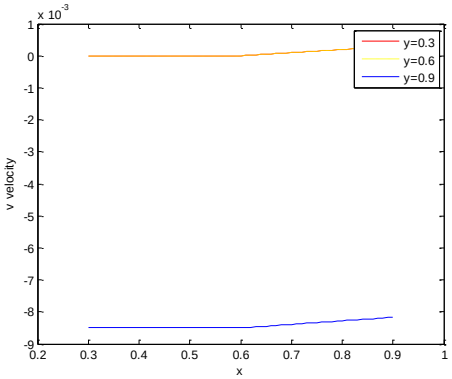

Fig. 13: v-velocity at t=0.020

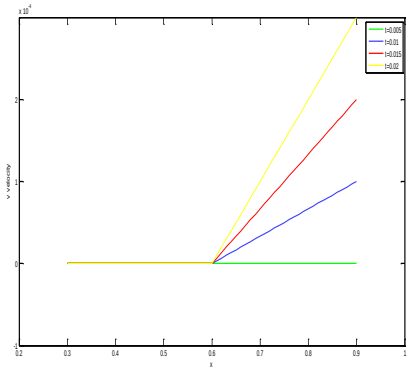

Fig. 14:v-velocity at y=0.3

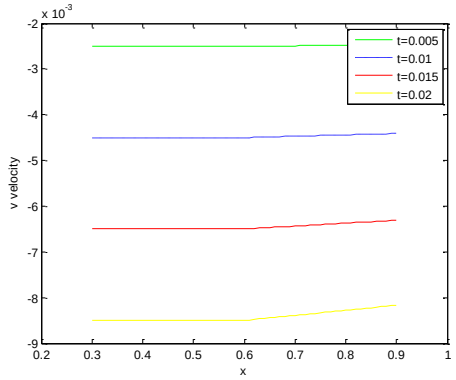

Fig 15 : v-velocity at y=0.9

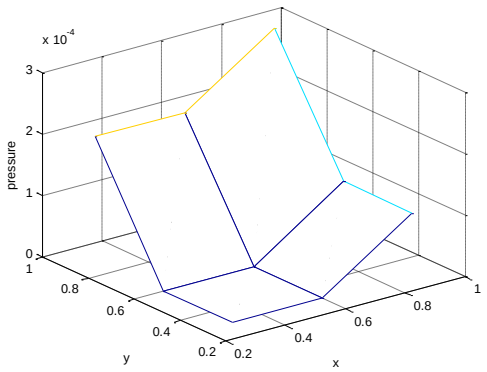

Fig. 16: Pressure at t=0.005

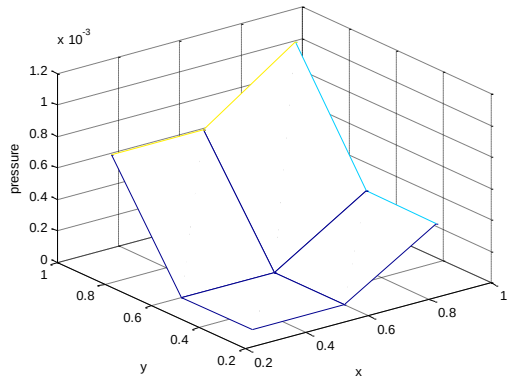

Fig. 17: Pressure at t=0.010

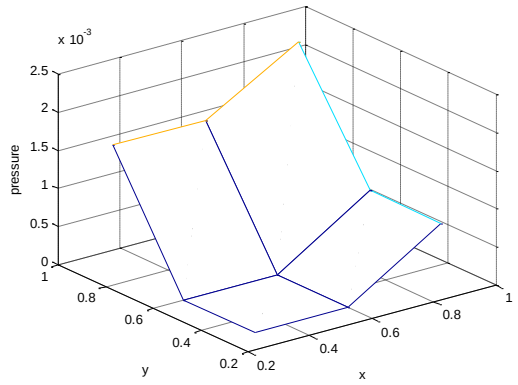

Fig. 18: Pressure at t=0.015

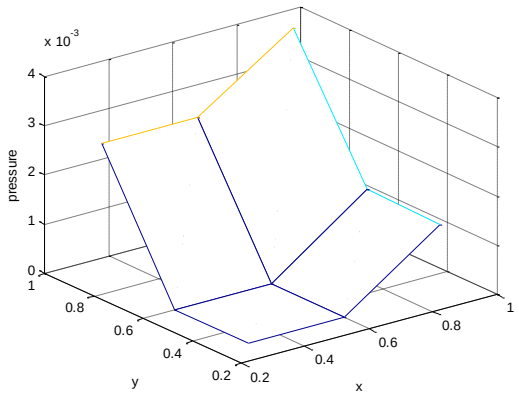

Fig. 19: Pressure at t=0.020

The numerical solutions for the temperature a different times 0.005, 0.010, 0.015 and 0.020 for values of *x* as 0.3, 0.6 and 0.9 and for values of y as

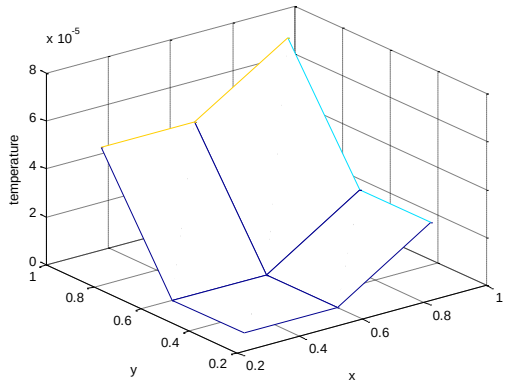

Fig. 20: Temperature at t=0.005

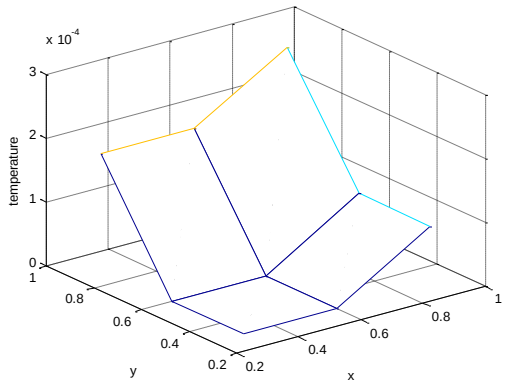

Fig. 21: Temperature at t=0.010.

0.3, 0.6 and 0.9 have been computed and given in Table 4.

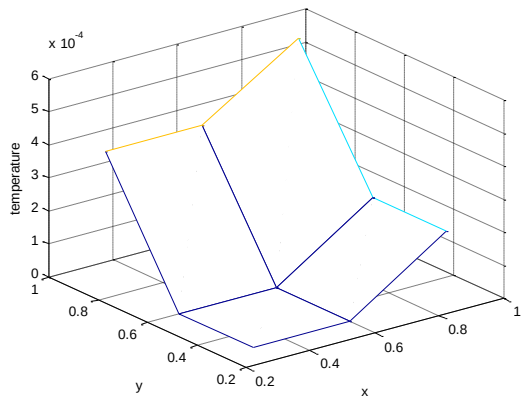

Fig.22: Temperature at t=0.015

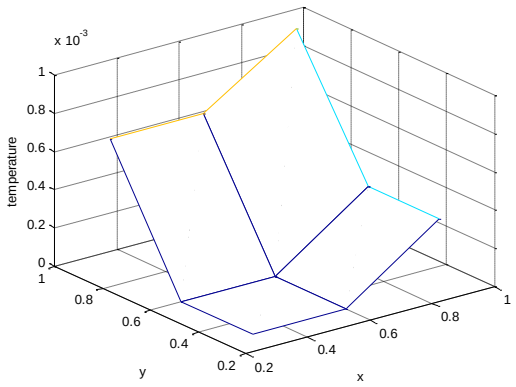

Fig. 23: Temperature at t=0.020

The pressure of the fluid at different times 0.0005, 0.010, 0.015 and 0.020 is illustrated in Figures 20 to 23.

V. RESULT AND DISCUSSION

From the numerical values of *u*-velocity of the fluid at different times 0.005, 0.010, 0.015 and 0.020 given in Table 1, it is observed that the *u*-velocity of the fluid along *y* axis increases steadily. But *u*-velocity at all time instants for different positions along *x*-axis (0.3, 0.6 and 0.9) for which the position of *y*-axis is 0.3, 0.6 and 0.9 decreases steadily. Same behavior can be seen in Fig. 4 to 7. The behavior of the *u*-velocity of the fluid at different times and different positions along *x*-axis has been illustrated from Fig. 8 and 9.It has been observed that *u*-velocity for y=0.9 increases as time passes for x=0.3 and x=0.6. For y=0.9, *u*-velocity decreases as time passes for x=0.9 only. In other words, the absolute value of *u*-velocity increases as time passes for different positions on *y*-axis.

The numerical values of *v*-velocity of the fluid at different times 0.005, 0.010, 0.015 and 0.020 are given in Table 2 and illustrated in Figures 10 to 13. It has been observed that for any fix value of *y* at a particular time, *v*-velocity increases for increase in value of *x*. This increase in *v*-velocity is more rapid as time progresses from 0.005 to 0.020.

From the numerical solutions for the pressure at different times given in Table 3 and illustrated in Figures 16 to 19, it has been observed that for fixed time and fixed values of *x*, pressure increases uniformly with increase in value of *y*. The same behavior is seen for increase in values of *x*, keeping fixed time and fixed value of *y*. Also, for particular values of *x* and *y*, it has been observed that the numerical values of pressure increases with increase in time from 0.005 to 0.020.

The numerical solutions for the temperature a different times 0.005, 0.010, 0.015 and 0.020 are given in Table 4 and illustrated in Figures 20 to 23. It has been observed that for fixed time and fixed values of *x*, temperature increases uniformly with increase in value of *y*. The same behavior is seen for increase in values of *x*, keeping fixed time and fixed value of *y*. It has also been observe that for all values of time for y=0.9, the temperature at x=0.9 is almost threefold of the temperature at x=0.3 or at x=0.6. We have observed that for particular values of *x* and *y*, it the numerical values of temperature increases with increase in time from 0.005 to 0.020.

VI. CONCLUDING REMARKS

The problem of an unsteady 2-D compressible inviscid flow with heat transfer with slip boundary conditions was investigated. Numerical solutions of governing equations are obtained using MacCormack technique. The numerical computations for *u*-velocity, *v*-velocity, pressure and temperature were conducted using a structured grid system. These numerical computations were performed using MATLAB programming language. Conclusions of this study are as follows:

1. The *u*-velocity of the fluid along y axis increases steadily. But *u*-velocity at all time instants for different positions along *x*-axis (0.3, 0.6 and 0.9) for which the position of *y*-axis is 0.3, 0.6 and 0.9 decreases steadily. Also, the absolute value of *u*-velocity increases as time passes for different positions on *y*-axis.

2. For any fix value of *y* at a particular time, *v*-velocity increases for increase in value of *x*. This increase in *v*-velocity is more rapid as time progresses.

3. For fixed time, both keeping *x*-fixed and *y*-varies or keeping *y*-fixed and *x*-varies, the pressure increases uniformly. Also, for particular values of *x* and *y*, it has been observed that the numerical values of pressure increases with increase in time from 0.005 to 0.020.

4. For fixed time and fixed values of *x*, temperature increases uniformly with increase in value of *y*. The same behavior is seen for increase in values of *x*, keeping fixed time and fixed value of *y*. Also, for particular values of *x* and *y*, it the numerical values of temperature increases with increase in time from 0.005 to 0.020.

Table 1: Numerical solutions for u-velocity

x	**y**	**u(t=0.005)**	**u(t=0.010)**	**u(t=0.015)**	**u(t=0.020)**
0.3	0.3	0	0	0	0
0.6	0.3	0	0	0	0
0.9	0.3	-0.002500014999	-0.004500049499	-0.006500103997	-0.00850017849
0.3	0.6	0	0	0	0
0.6	0.6	0	0	0	0
0.9	0.6	-0.002500014999	-0.004500049499	-0.006500103996	-0.008500178489
0.3	0.9	0.0000250001624	0.00009000106497	0.00019500334724	0.000340007648
0.6	0.9	0.0000250001625	0.00009000106499	0.00019500334744	0.000340007649
0.9	0.9	-0.002475128177	-0.004411013995	-0.006308389216	-0.008167971198

Table 2: Numerical solutions for v-velocity

x	y	v(t=0.006)	v(t=0.01)	v(t=0.014)	v(t=0.018)
0.3	0.3	0	0	0	0
0.6	0.3	0	0	0	0
0.9	0.3	0.0000250001624	0.0001	0.0002	0.0003
0.3	0.6	0	0	0	0
0.6	0.6	0	0	0	0
0.9	0.6	0.0000250001625	0.0001	0.0002	0.0003
0.3	0.9	-0.002500014999	-0.004500049499	-0.0065001039972	-0.008500178490
0.6	0.9	-0.002500014999	-0.004500049499	-0.006500103997	-0.008500178489
0.9	0.9	-0.002475128177	-0.004411013995	-0.0063083892168	-0.008167971198

Table 3: Numerical solutions for Pressure

x	y	p(t=0.005)	p(t=0.010)	p(t=0.015)	p(t=0.020)
0.3	0.3	0	0	0	0
0.6	0.3	0	0	0	0
0.9	0.3	0.0002	0.0007	0.0016	0.0027
0.3	0.6	0	0	0	0
0.6	0.6	0.000100001019998	0	0	0
0.9	0.6	0.0002	0.0007	0.0016	0.0027
0.3	0.9	0.000100001019997	0.00036000659985	0.0007800206426	0.0013600470493
0.6	0.9	0.000100001019984	0.00036000659988	0.0007800206429	0.0014000470509
0.9	0.9	0.0002985	0.0011	0.0023	0.0040

Table 4: Numerical solutions for Temperature

x	y	T(t=0.005)	T(t=0.010)	T(t=0.015)	T(t=0.020)
0.3	0.3	0	0	0	0
0.6	0.3	0	0	0	0
0.9	0.3	0.00005	0.00018	0.00039	0.00068
0.3	0.6	0	0	0	0
0.6	0.6	0	0	0	0
0.9	0.6	0.00005	0.00018	0.00039	0.00068
0.3	0.9	0.00002500019	0.00009000124498908	0.0001950038933965	0.000340008873507
0.6	0.9	0.00002500019	0.00009000124499134	0.0001950038934151	0.000340008873594
0.9	0.9	0.00007463	0.0002669	0.0005744	0.0009949

REFERENCES

[1]. R.W. MacCormack,"*The effect of viscosity in hypervelocity impact crartering*", AIAA paper, pp. 69-354, 1969.

[2]. Robert S. Bernard, "*A MacCormack scheme for incompressible flow",* Computers and mathematics with applications, Vol. 24, Issue 5-6, pp 151-168, 1992.

[3]. F. Payri, A.J. Torregrosa and M.D. Chust, "*Applicationof MacCormack scheme to IC engine exhaust noise prediction*", Journal of sound and vibration, Vol. 195, Issue 5, pp 757-773, 1996.

[4]. R. Hixon and E. Turkel," *High accuracy compact MCT scheme for computational acoustics*",36 Aerospace Sciences Meeting and exhibition, Reno, NV. 1998.

[5]. R. Hixon and E. Turkel," *Compact implicit MC type scheme with high accuracy",* Journal of computational physics, Vol 158, Issue 1, pp. 51-70, 2000.

[6]. A.Perrin and H.H.Hu,:*An explicit finite difference scheme for simulation of moving particle*", Journal of computational physics, Vol. 212, Issue 1, pp 166-187, 2006.

[7]. Li Guoyuan and C. Rhett Jackson,"*Simple, accurate andefficieny revisions to McCormack and Saulyev Schemes: High Peclet number",* Applied mathematics and Computations, Vol. 186, Issue 1, pp 610-622. ,2007.

[8]. Noppart Pochai, "*Numerical treatment of a modified MacCormack scheme in a non dimensional form of water quality models in a non uniform flow stream",* Journal of applied mathematics, Vol. 2014. Article ID 274263

[9]. Samir K. Das and Jafar Bagheri," *Modeling of shallow water equations by using compact MacCormack type scheme with applications on dam break problem",* International Journal of Advance Applied Mathematics and Mechanics Vol. 2 ,Issue 3, pp 60-71, 2015.

[10]. T.P. Gallagher, M. Akiki, S. Menon, V. Sankaran, V. Sankaran," *Development of generalized MacCormack scheme and its extension to low mach number flows*", International Journal for numerical methods in fluids. Vol. 85, Issue 3, pp 165-188. 2017.

[11]. J. D. Anderson,"*Computational Fluid Dynamics: The Basics with Applications",* McGraw-Hill Publications, First(Ist) Edition, April 1995.

[12]. H.K. Versteeg, W. Malalsekra, "*An Introduction to Computational Fluid Dynamics: The Finite Volume Method*", Prentice Hall, Second (2nd) Edition, February 2007.

[13]. Prabhjot Singh and Anjana Sharma*," Face Recognition Using Principal Component Analysis in MATLAB*", International Journal of Scientific Research in Computer Science and Engineering, Vol.3, Issue 1, pp.1-5, 2015.

AUTHOR'S PROFILE

Dr. Arti Kaushik has been associated as Assistant Professor with Department of Mathematics, MAIT, Delhi for last 12 years. She is an ardent researcher. Her research interest includes Fluid Dynamics and Computational Fluid Dynamics. She has published many research papers in national and International Journals of repute.

